

The development and test research of multi-channel Synchronous transient electromagnetic receiver

Fanqiang Lin ^{1,2}, Xuben Wang ^{2,3}, Kecheng Chen ¹, Depan Hu ⁴, Song Gao ¹, Xue Zou ¹, and Cai Zeng ¹

¹College of Information Science and Technology, Chengdu University of Technology, Chengdu 610059,China

²College of Geophysics,Chengdu University of Technology, Chengdu 610059,China

³Key Lab of Geo-Detection and Information Techniques of Ministry of Education, Chengdu 610059,China

⁴Geoenvironment Monitoring Institute in Chengdu, Chengdu 610071,China

Correspondence: Fanqiang Lin(linfq@cdut.edu.cn)

Abstract. As a result of the drastic reduction of shallow mineral resources, the exploitable potential and reserve of proven mines ~~have been proven~~are insufficient, and the mineral resources in deep ground need to be more refinedly explored.~~Because~~
~~There are some disadvantages~~ of the existing instruments~~have less channels and insufficient~~, such as few channels and slow
sampling rate, ~~the development and experiment of the etc.~~ Therefore, multi-parameter transient electromagnetic instrument
5 with ~~multi-channel synchronous receiving are therefore proposed~~synchronous receiving has been developed and tested. The
instrument is composed of two controllers, embedded controller and programmable logic controller, which can provide di-
versified information combination. Under the grounding electrode source emission mode, the real-time synchronous transient
electromagnetic acquisition system ~~in six channels of six channels is achieved~~ with 128k sampling rate ~~is achieved~~. The data
of the six channels are recorded in the full time range in the time domain. At the same time, experiments were carried out
10 in laboratory, open areas and actual mine. Through data analysis, the measured data curves of the mining area ~~is are~~ highly
consistent with the existing geochemical exploration curves and geological profile.

1 Introduction

Transient electromagnetic method belongs to the active field source method of time domain electromagnetic method. The prin-
ciple is that the conductive geological body existing underground produces induced eddy currents under the action of alternating
15 electromagnetic fields, and the eddy current further generates secondary magnetic fields. In transient electromagnetic method,
~~it often using~~ periodic bipolar waves ~~as the launch signal, are used as launch signals, and~~ data acquisition is completed during
the bipolar wave ~~intermittent~~intermittence, thus effectively avoiding the coupling problem in the frequency domain electromag-
netic method. The instrument collects and studies the decay characteristics of the intensity of each component, distribution,
space and time ~~decay of the second field, and then deduces of~~ the secondary fields to deduce the underground anomalies. The
20 transient electromagnetic signals contain very rich frequency components, which ~~are very useful for~~ can easily penetrate low-
resistivity geologic bodies~~with high penetration, which can effectively improve, and therefore~~ the actual exploration depth can
be effectively improved.

Conventional transient electromagnetic (TEM) ~~use~~uses mostly magnetic source or electrode source mode. ~~In~~ the magnetic source mode TEM volume effect is relatively small, ~~and it has~~ high detection accuracy, but the effective detection depth is usually less than 500 meters, and the ~~high-Geological-response~~response to high resistivity geological bodies is not sensitive. However, LOTEM can increase the exploration depth up to 10 km. However, due to the large distance between the LOTEM transmission and reception, the accuracy of the collected data is relatively low, as well as a poor ~~signal-to-noise-ratio~~signal to noise ratio(SNR) and increased possibility of interference on the way of long-distance transmission(Brunke et al.,2017). As a result, domestic scholars such as Xue Guoqiang proposed short offset transient electromagnetic (SOTEM) device method(Xue et al.,2013,Chen et al.,2016,Chen et al.,2017), the ~~reduce~~reduction of transceiver distance can both greatly enhance the exploration depth, but also effectively improve the ~~signal-to-noise-ratio~~SNR. In recent years, it has a very broad application prospect in such fields as engineering environment, geological disaster investigation, underground gob area, groundwater, petroleum, coal and other non-metallic mineral exploration and advanced geological prediction.

2 Literature review

In 2010, internationally renowned geophysicist Zhdanov proposed the following directions for future electromagnetic exploration instruments and methods in the 75th anniversary of "Geophysics": Multi-component emission, Multi-channel reception and Pseudo-seismic data collection (Qi et al.,2015,Ayuso et al.,2016). As the demand for resources and energy increases due to economic development, the depth is increased to the second depth space (500-2000m) on the basis of the existing exploration depth (500m depth range). The fine exploration within this range will be a long-term and heavy task to study new theories and methods and to develop equipment with higher adaptability to make up the lack of traditional exploration methods and instruments.

China's overall theoretical level and engineering practice in the field of transient electromagnetic remain at the ~~same-level with the international~~, ~~but~~international level, but compared with foreign instrument, the domestic instruments still have some disadvantages in the technical indicators~~comparing with foreign countries there is still a certain gap~~, which will be constraining China's original innovation and quantitative calculation of the bottleneck(Zhong et al.,2016,Zhang et al.,2017). With the development of electrical prospecting theory, instrument's design and development, many kinds of instrument products have been made. The main development directions are automation, intelligence, refinement and lightness. As a result, various institutions of higher learning and research institutes in China have introduced various forms of transient electromagnetic prospecting instruments in their decades of development. By comparing most of the transient electromagnetic surveys at home and abroad ~~since in~~ recent 20 years, the main problems ~~and gaps in~~of the domestic transient electromagnetic instrument lie in that: some technical indicators are lagging behind; the function is insufficient; the consistency is low and so on. It can be seen that the development of new acquisition devices, the transformation of new launch modes, acquisition methods, the development of new instruments and evaluation methods of electromagnetic methods, etc. are particularly important(Li et al.,2012). The core of this paper is to develop a receiver system for synchronous acquisition of multiple electromagnetic signals in transient electromagnetic prospecting to achieve multi-parameter and multi-channel synchronous reception. High-speed programmable

logic devices are used to achieve high-level synchronization between channels. ~~Waveform-Transmitting current waveform~~ acquisition and multi-channel ~~receive-reception can be synchronized~~ by using high-precision GPS timing unit ~~to-synchronize,~~ ~~combined-with,~~ and programmable high-precision counter ~~is adopted~~ to further improve the synchronization accuracy.

3 ~~Multi-channels~~ Multi-channel receiver hardware and software design

3.1 Receiver framework

Receiving system consists of four parts, namely: FPGA unit, ARM unit, analog acquisition unit and power supply circuit.

10 System block diagram shown in Figure 1. Analog board channel numbers are 1/2, 3/4, 5/6 channels respectively, and each analog board have two channels. The board ~~contain-contains~~ the signal conditioning circuit, amplification and acquisition of all channels which are completely independent ~~and-~~, and multi-channel real-time synchronized acquisition is achieved ~~in~~ multi-channel.

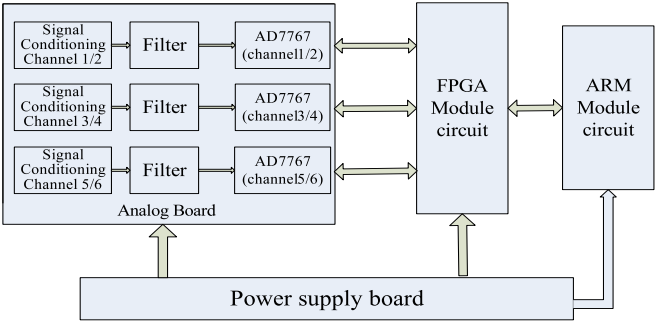


Figure 1. System block diagram of hardware

15 3.2 Design of analog circuit board

Analog board mainly includes signal conditioning (including: the first stage instrumentation amplifier, the second stage programmable amplifier, low-pass filter), protection circuit (positive and negative polarity of each input stage clamp diode), the natural potential compensation circuit(Liu et al.,2016), single-end to differential circuit and analog to digital converter.

The first stage amplifier uses a dedicated high-precision, low-noise INA114, and using the AD5272 high-resolution digital potentiometer to design the precision gain op-amp, to achieve high-precision amplification and range adjustment. The two circuits are shown in Figure2 and Figure3.

20

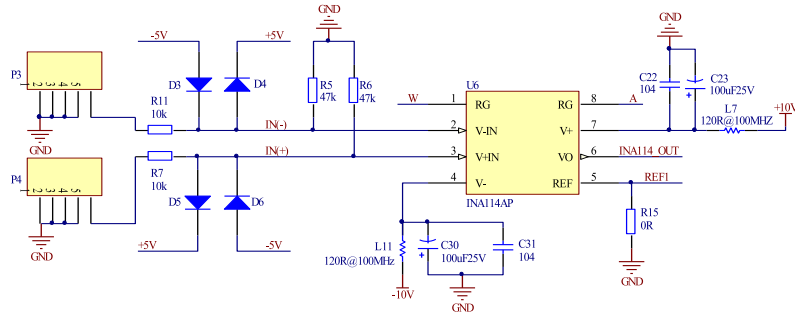


Figure 2. INA114 instrument amplifier circuit

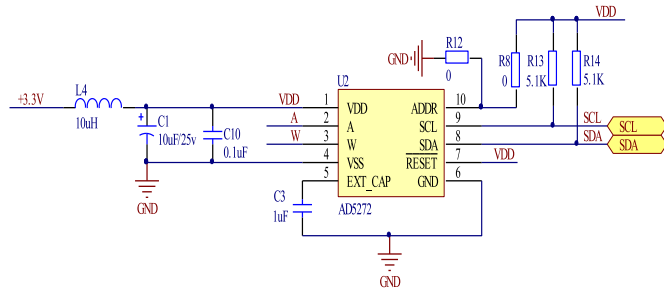


Figure 3. AD5272 Digital potentiometer

It utilizes the PGA103 program-controlled amplifier, making use of and a general IO port to complete the three level amplification ratio adjustment.

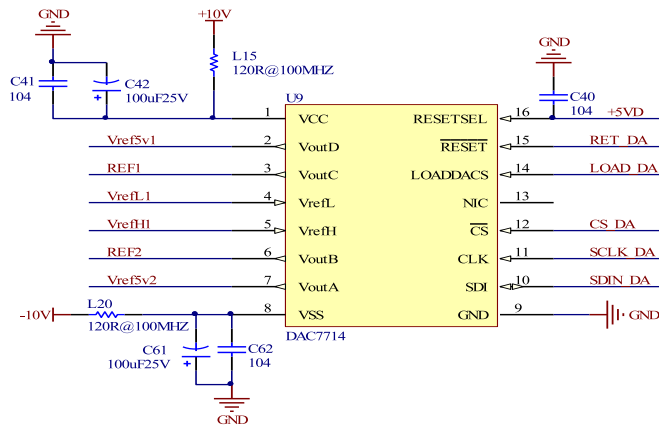


Figure 4. DAC7714 compensation and Vref circuit

nel,~~reducing to reduce~~ noise from the front end and ~~reducing~~ the need for front-end anti-alias filter, ~~which using a and~~ daisy chain technology to realize the multi-chip ~~series~~ cascade connection for an efficient parallel ~~device~~ synchronous acquisition (Liu et al.,2017).~~The design of the two channels as a result of a~~ The two circuits are shown in Figure5 and Figure6.



15 By adopting modular design, ~~it is two AD7767 series, the FPGA controller to control the three analog boards by three connectors, and then through the FPGA internal logic program, the six channels are the~~ chips are cascaded. FPGA controller is used to control three analog circuit boards separately, and the overall data package and storage in real-time ~~is achieved.~~

3.3 Design of digital logic controller board

Multi-channel synchronous receiver ~~with uses~~ embedded controller and programmable logic controller (FPGA) ~~in as~~ dual-
20 controller ~~approach~~(Oballe-Peinado et al.2017) , ~~this control method which~~ is flexible and ~~more popular widely~~ used. FPGA ~~as the core is the core logic control~~ part of the ~~system to collect the front end of the logic control components for the main use of its internal parallel processing functions, collection system, and the synchronization between the various functional units can be easily achieved by its parallel processing function, by which a number of internal logic modules logic modules are driven by the system clock, you can easily achieve the synchronization between the various functional units.~~This instrument uses the
25 XC6SLX9 chip ~~that belongs as the core acquisition controller, that belongs to~~ the Spartan-6 ~~family series~~ of well-known FPGA chip maker Xilinx.FPGA unit ~~module~~ is mainly composed of SD card unit circuit, SRAM buffer circuit and the SPI interface which is used to communicate with STM32 controller.~~It is responsible for,~~ the synchronous acquisition and control interface of ~~6 six~~ channel signals, filter frequency output interface, and GPS's second-pulse signal interface, and power interface.

30 The embedded control unit adopts the STM32F4 series of ST Microelectronics which is popular in industry. The embedded control part has completed the functions of keyboard ~~, and~~ FPGA communication control interface, GPS location information collection and liquid crystal display. The embedded unit ~~communicate communicates~~ with the FPGA controller by SPI interface. It also collects the GPS time information, such as latitude and longitude, etc. which is outputted by the GPS module through the serial port, and simultaneously ~~displays it displayed~~ on LCD. ~~The system also designs a~~ 6*8 matrix keyboard ~~which can is designed to~~ set some parameters of the system. When the GPS satellite signal is locked, the receiving system can
5 collect the data according to the preset instruction by start key. Both ~~of selecting of selecting~~ the channel for collection and setting the channel on or off can be finished with the LCD and keyboard control in actual work.And ~~it using~~ general purpose IO port ~~is used~~ to control DAC7714 chip ~~, which can be used~~ to achieve natural potential compensation and fine gain tuning.~~The logic core diagram is shown in figure7, and the STM32F407 diagram is shown in figure8.~~

10 3.4 Design of high-precision linear power circuit

After comparing the multi-output power supply circuit board designed by the switching power supply module, a Low Drop Out linear power chip with high precision and high ripple rejection is selected(Joo et al.,2017,Duong et al.,2017). On the power supply board, three independent connecting plugs are used to supply power to each analog board(Ren et al.,2015). Here, the high-reliability TPS7A ~~family series~~ of voltage regulators designed by Taxi Instrument ~~which~~ features wide input voltage

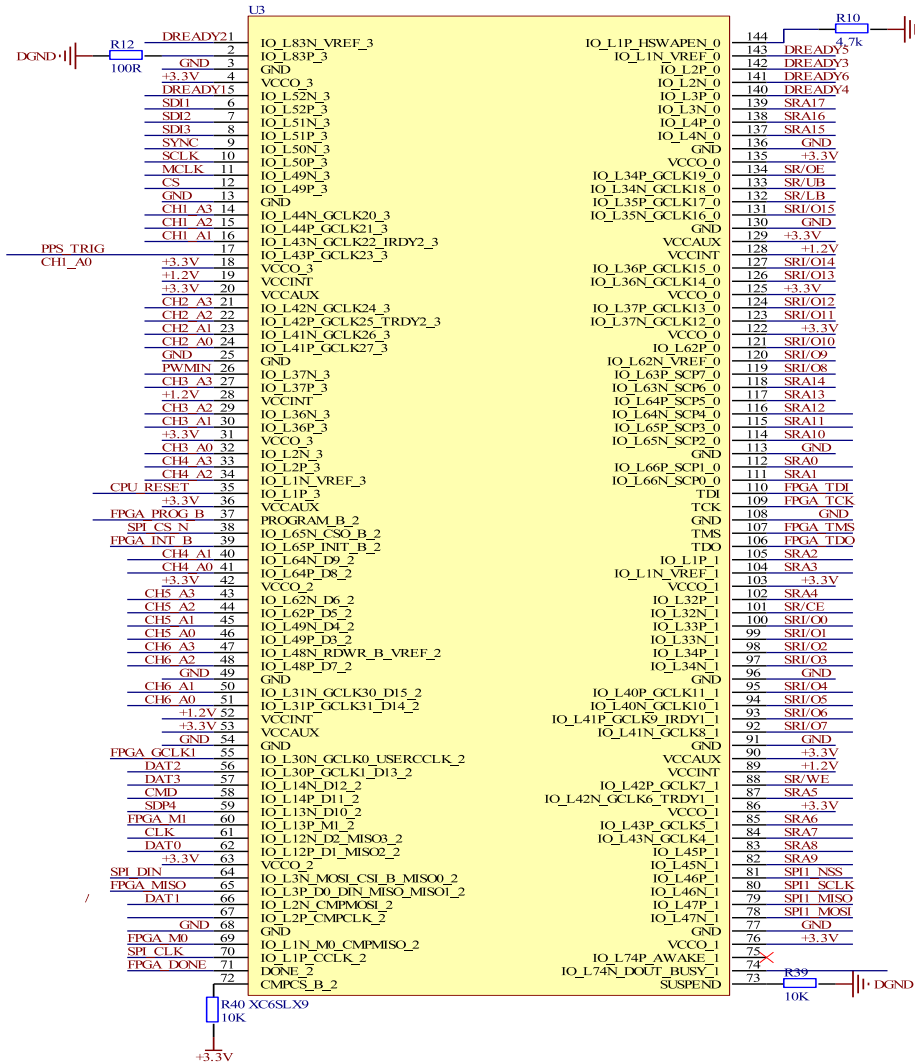


Figure 7. XC6SLX9 FPGA circuit diagram

15 range, low noise, and high supply ripple rejection is selected. The power board have has 4 different voltage output: + 10V, -10V, + 5V, -5V for preamplifiers and filters. Another separate + 5V power supply for digital potentiometers on analog board and DAC7714, etc., and a 3.3 V Power provides digital logic power for Analog-to-Digital converter AD7767(Yun et al.,2017).The high precision and high power supply rejection rate diagram is shown in figure9.

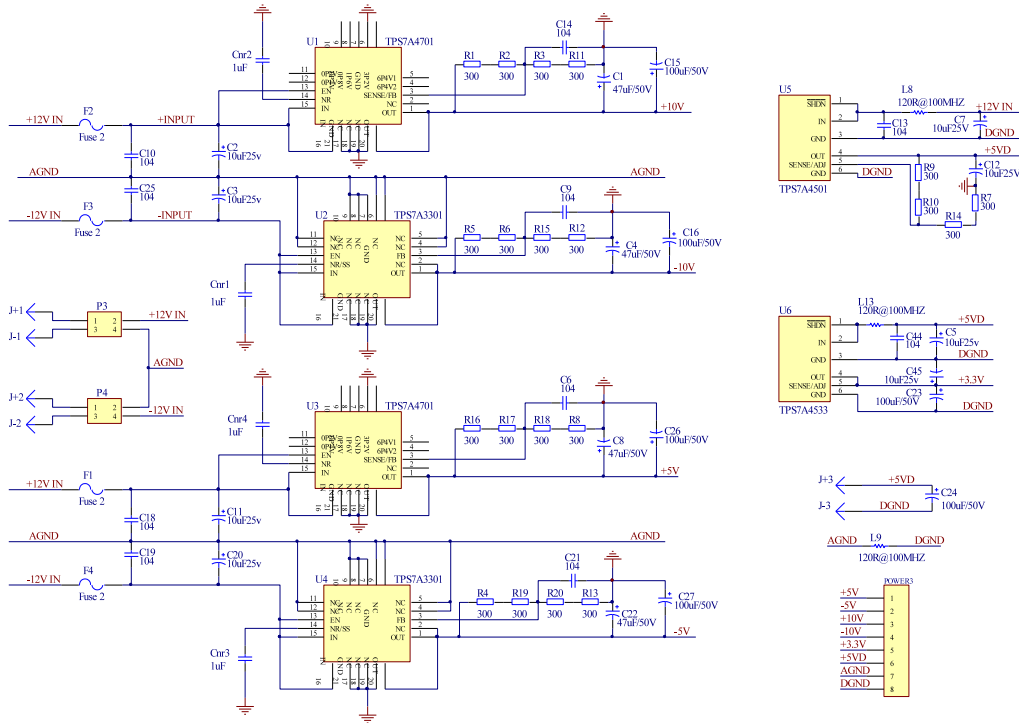


Figure 9. Linear power circuit diagram

number-together-for-the-later-storage numbers are stored in a package through FPGA program. Those information is stored in the first 8 bytes of each sector in SD card. GPS-timing-unit-provided-by-the-The second pulse signal(PPS) ,FPGA-synchronize the-transceiver-provided by GPS timing unit updates the internal base time of FPGA in every two seconds. It can reduce the cumulative-error-in-long-time-collectiontime cumulative error.

Embedded controller is responsible for coordinating the work-operation of the entire system, such as the system gain adjustment of each channel, GPS time information reception and status monitoring, real-time data-acquisition-and-display-of information,and-FPGA-controller-communicationdisplay of acquired data,and interface communicating with FPGA controller(Zhang et al.,2017).

5 4 Performance test

Performance test of the receiver system mainly include-includes DC testing, AC testing and field testing(Ziolkowski et al.,2010,Zhou et al.,2015).In the DC stability test, we first test the magnification range of each channel and the magnification consistency. Taking the first channel as an example, as shown in Figure 2-11 below, the input signal is a blue curve with a

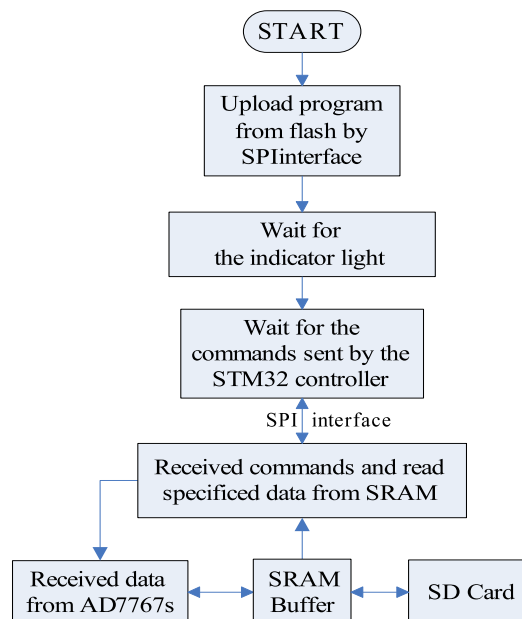


Figure 10. Flowchart of system program

Table 1. Magnification test of each channel

Channel No.	Magnification mean
Channel 1	94.42
Channel 2	94.46
Channel 3	94.39
Channel 4	94.68
Channel 5	94.32
Channel 6	94.59

range of $\pm 50\text{mV}$. The red curve is the magnification curve of the first channel when each input signal is calculated. According to Under the same test conditions, the six channels are connected in parallel, under and the same input signal conditions, the acquisition of signals are received by six channels at the same time, the average magnification. The average magnification times of each channel are shown in Table 1, the portion of the difference between each channel is small. 1.

Next is the conformance test between channels for of the receiver. The test is to better maintain a high degree of high consistency between channels. The test project is: Sequence the seven connection In the test, positive terminals of the six channels , with the odd-numbered terminals connected together and the even-numbered terminals connected together. After connecting in this way, two terminals appear, that is: the common terminal of the odd terminal and the common terminal of the

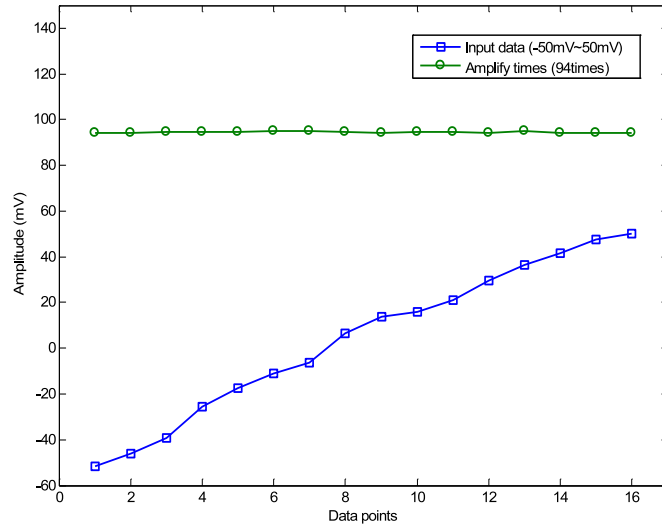


Figure 11. First Channel DC Test

Table 2. Error analysis table of inter-channel consistency

Channel No.	Group1(mV)	Group2(mV)	Group3(mV)	Group4(mV)	Average(mV)	Average Error(mV)	Error Percentage(%)
Channel 1	20.7398	20.7372	20.7382	20.7359	20.7378	0.0020	0.1901
Channel 2	21.0451	21.0465	21.0510	21.0465	21.0473	0.0022	0.3432
Channel 3	20.7961	20.7927	20.7938	20.7964	20.7948	0.0013	0.1328
Channel 4	21.0050	21.0044	21.0057	21.0015	21.0042	0.0008	0.2303
Channel 5	21.0529	21.0504	21.0500	21.0530	21.0516	0.0013	0.0282
Channel 6	20.8906	20.8911	20.8906	20.8914	20.8909	0.0004	0.2013

even-terminal-are-connected-with-the-are connected together, while the negative terminals are connected with each other. The two connected terminals are input with standard sine waves signal, the- The amplitude of the input signal is 20mV peak-to-peak and the frequency is 150Hz. For the same point in time, the extraction of the value of each channel- The extracted numerical values of each channel at the same time are compared to obtain the average of each-channel-error, the average absolute error and error percentage, as shown in Table 2.

In the AC testing, the six channels of positive and negative parallel-are access to the sine wave-terminals are connected in parallel, and the sine waves are input from the standard signal source. The waveform output by the system after the acquisition is-output waveforms after the system acquisition are shown in Figure 3, the input signal peak-10mV, frequency of-12. The peak to peak value of input signal is 10mV, and the frequency is 20Hz. As can be seen from the figure, each-channel-has-high consistency-the consistency between each channel is quite high and no phase offset occurs. After the system-is-enlarged, each

channel-waveform-shows-peak-to-peak-input signals are amplified by the system, peak to peak value displayed by waveforms of each channel reaches to 1000mV through amplifier.

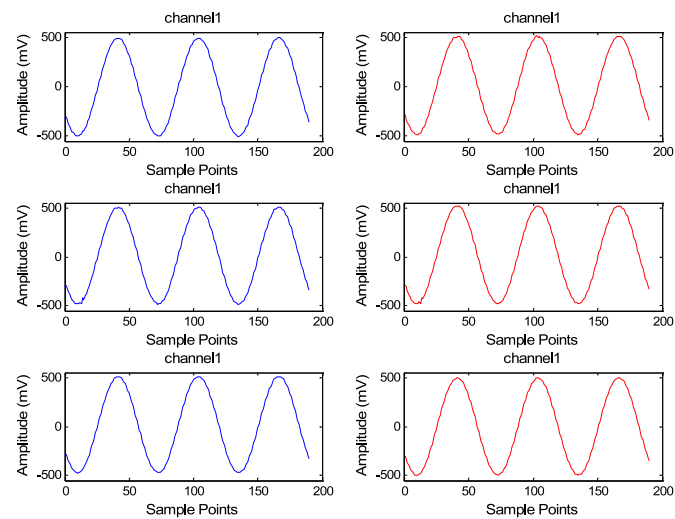


Figure 12. Standard sine wave of six channels in synchronous receiving

Figure 4 is the first channel in Figure-In Figure 13, the left figure is about the waveform of 3 ,by cycles of data acquisition by the first channel shown in Figure 12. The right figure is about the frequency spectrum formed by waveforms in the left one, which underwent fast fourier transform,it can be seen from the frequency spectrum of the sine wave in the left time domain, and-. As is shown in the right one, the frequency of the input sines waves is 20Hz, with few harmonic componentsin the right frequency domain, which indicates the excellent performance of analog circuit board and high stability of power circuit.

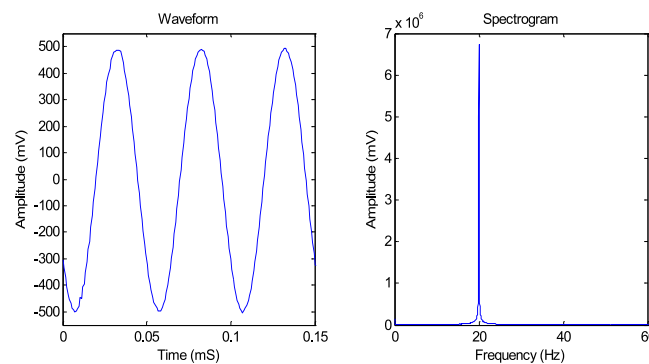


Figure 13. AC-test waveform and its spectrum diagram in AC test

5 Field testing

In the field testing, ~~sensor is~~ a hollow coil with ~~400 turns and it's diameter is 400 turns and a diameter of~~ 50cm ~~, the effective area of the coil is used as the test sensor, and its effective area is~~ $40m^2$. The transmitter ~~uses is~~ Phoenix's T-4 transmitter, which transmits a bipolar pulsed ~~waveform~~ numbered TD50 with a 50% duty cycle(Wang et al.,2015).

- 10 Two sites were selected, ~~the first one one of which~~ is a relatively open site ~~and the second one while the other~~ is the actual mining area. ~~The test uses a near-field measurement method . The transmitting source of the field adopt grounded electrode~~ Near-field measurement method is used in the test. Grounded electrode source is adopted as the field source. Four aluminum plates ~~as electrodes~~ are respectively buried ~~40cm deep~~ in the ground ~~with 40cm of aluminum plate~~ and covered with salt water and soil, so that the grounding resistance is less than 10 ohms. The ~~spacing of distance between~~ the transmitting electrodes ~~is~~ 300 meters, the power supply using four batteries , voltage control A and B is 400 meters, and the four batteries are used as the
- 5 ~~power supply. The voltage ranges~~ between 40-50V, ~~while~~ the emission current ~~of is~~ 3A, and the ~~launch frequency of emitting frequency is~~ 25Hz.

- During the test, the power supply ~~electrode is electrodes are~~ stationary, while the preset measurement ~~and emission level is at an offset of line is parallel with the emission points A and B. The offset is~~ 40 meters. ~~During the test, two machines were used, one of them is used to record the emission current waveform and the other is used to receive the voltage of the~~ The changing
- 10 ~~rate of the~~ magnetic flux density (dB/dt) ~~at the preset point. Figure 5 is received by the coil. Figure 14 below shows the original one-cycle data one original one cycle.~~

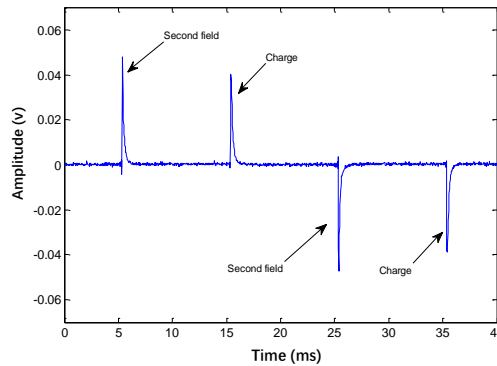


Figure 14. ~~single-cycle (40mS) secondary field and a field single cycle~~ waveform

The open area ~~to be tested where the test was carried out,~~ is formed by the ~~mixing and filling mixture~~ of soil and slag. Each ~~survey line was measurement line~~ observed at 8 ~~measuring~~ points. After the data was stored, it was processed by computer program written in MATLAB and the secondary field information of each measuring point was extracted and processed. The following ~~two profile curves were profile curve was~~ formed.

5 Figure 6 shows the cross-section of this line. The cross-section 15 shows the profile, which shows that the overall response tends to be flat. The difference between the two launch points is due to the close proximity of the emitter point received by the signal is signals received at the measurement points close to the transmitting nodes are relatively strong, closer to the middle, the profile line slowly flat while the central part of the profile becomes flat slowly.

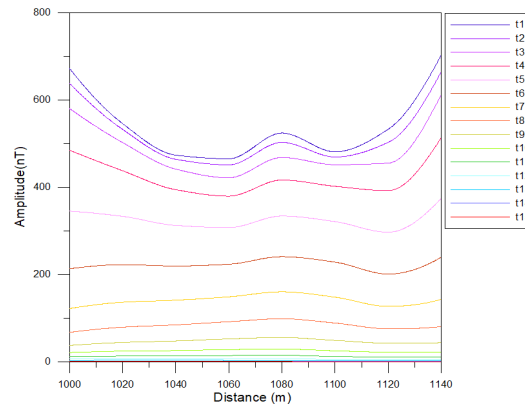


Figure 15. Close to the source L1 line profile

In order to test the performance of the receiver further, a mining area in Leshan, Sichuan Province was selected for the forth field test, and a relatively gentle geodetic survey line was planned. The use of electrode source emission, emitter distance of is adopted, and the distance between the transmitting electrodes stance is 400 meters. The testing line offset is 80 meters, measuring point spacing of and the distance between the measuring points is 40 meters.

Mining area test is still using a A continuous launch mode is used in mining area test, and the transmission signal frequency is 25Hz. Figure 7-16 is a waveform of the two periods two cycles of the raw data collected in the mining area. Compared with Figure 6, it can be clearly seen that there is a big difference in the magnitude of the change of the magnetic induction between the secondary field and the charging due to the fact that the area is a metal mine, Less heat loss of electromagnetic waves.

The second-field extraction, filtering and interpolation are performed on the data collected After the collected data in the mining area. After 200 superimposed waveforms, the waveform are second-field extracted, filtered and interpolated, the waveform is formed. The waveform curve of the time domain is smoother, after, 200 superimposed waveforms, which can well reflect the response of underground media geological bodies to transient electromagnetic. The data of each measuring point are processed in the same way to obtain the pure secondary fields field curves, and the time sampling is performed to form a sectional view domain order waveforms are extracted to form the profile of the measuring line. In Fig. 8, t1~t12 respectively represent the extraction time, and connect the extracted values of different collection points are collected together to form 12 curves at different times.

As can be seen from the comparison of Figures 9 and 10 with Figure 8 by comparing figure 18 and figure 19 with figure 17, the high anomaly point is near by 1160 test point test point 1160, which happens to be a sloped metal vein. Thus it is verified that the receiver can acquire the signal of transient electromagnetic emission very well. By analyzing and comparing the profile

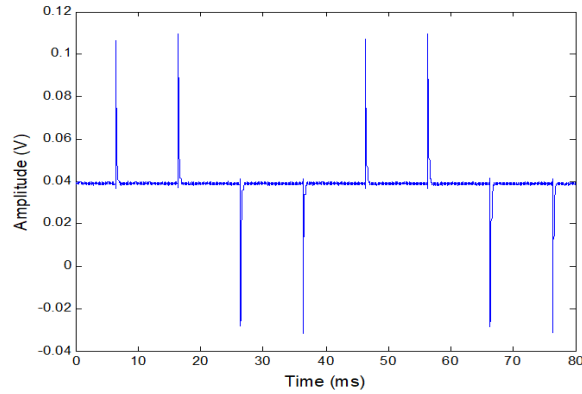


Figure 16. Waveform diagram acquired in mining area(two-eyeles)

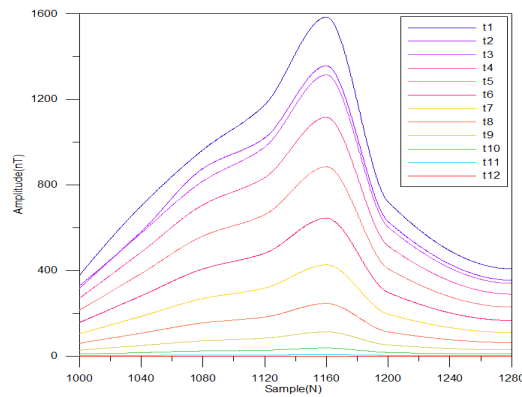


Figure 17. Survey line profile of copper mining area

and the measured with the actual geochemical distribution, it can be obviously seen that the abnormality of the curve-curves is highly consistent near +160 point- point 1160. In addition, the anomaly is more in line consistent with the geological structure in this area.

20 6 Conclusions

The purpose of this paper is to develop a set of receiver device that can adapt to application of be applied in transient electromagnetic prospecting. First, the hardware circuit and software program-circuits and software programs are designed to realize all functions which are presented above. By means of dual controller, the instrument can receive six-channels signal synchronously-signal synchronously through six channels. Then, the data stored in SD card is-are processed by computer program and generate-graphic programs to generate graphs. The overall performance was tested, All the channels reached an error of of the receiver was tested and verified. All the collected data error of each channel is less than 0.35%, and, each channel

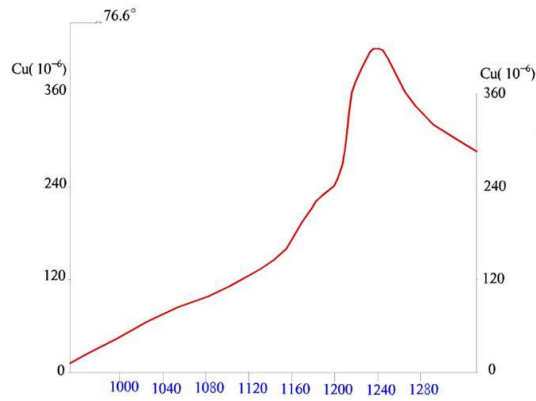


Figure 18. Geochemical Anomaly of geochemical exploration of copper area along the survey line

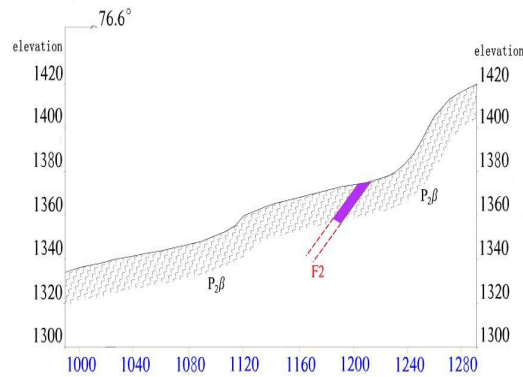


Figure 19. Geological profile of mining area

can connect different sensors, such as coil, magnetic probe, electrode. This kind of receiver can be used to collect transient electromagnetic information acquisition. It has high precision. Due to its high precision and high sampling rate, it can capture the fast falling edge of TEM, ultra-low noise and soon ultralow noise and so on. Hence, the multi-channel synchronous acquisition of magnetic field information in three directions and electric field information in two directions and the rate-of-change-of changing rate of magnetic induction intensity can be used for time domain reception. Meanwhile, pseudo-Random-the receiver can be used for pseudo random signal reception and distributed 3D-reception provide strong support for further exploration of different ways.

3-dimension data reception, which can improve geophysical exploration efficiency.

35 Code availability. The code of the receiver are available upon request(linfq@cdut.edu.cn)

Data availability. The circuit schematics of the receiver are available upon request(linfq@cdut.edu.cn)

Appendix A

A1

Author contributions. FQ developed the main hardware and a part of software, XB instructed all the authors. And others participated in the experiments and software development.

5 *Competing interests.* The authors declare that they have no conflict of interest.

Acknowledgements. This work was supported by National key research and development project(no.2016YFC0600300),National natural science Foundation of China (NO.41674078),and Field observation and research base of ministry of land and resources of China for Geohazards in earthquake disturbed area of Longmen Mountain in Chengdu.

References

- 10 Ayuso, S., Blanco, J. J., Medina, J., Gomez-Herrero, R., Garcia-Poblacion, O., Gracia, T. I.: A coincidence detection system based on real-time software, *Geoscientific Instrumentation Methods and Data Systems.*,2,1-36, DOI: 10.5194/gi-5-437-2016,2016.
- Brunke, H. P., Widmer-Schmidrig, R., Korte, M.: Merging fluxgate and induction coil data to produce low-noise geomagnetic observatory data meeting the INTERMAGNET definitive 1 s data standard, *Geoscientific Instrumentation Methods and Data Systems.*,2:487-493. DOI:10.5194/gi-6-487-2017,2017.
- 250 Chen, W. Y., Khan, M. Y., Xue, G. Q.: Response of surface-to-borehole SOTEM method on 2D earth, *Journal of Geophysics and Engineering*, 3,987-997. DOI:10.1088/1742-2140/aa6fcc,2017.
- Chen, W. Y., Khan, M. Y., Xue, G. Q., Cui, J. W., Zhong, H. S.: Study on the response and optimal observation area for SOTEM, *Chinese Journal of Geophysics-Chinese Edition.*,2,739-748. DOI:10.6038/cjg20160231,2016.
- Duong, Q. H., Nguyen, H. H., Kong, J. w., Shin, H. S., Ko, Y. S., Yu, H. Y., Lee, Y. H., Bea, C. H., Park, H. J.: Multiple-
255 Loop Design Technique for High-Performance Low-Dropout Regulator, *IEEE Journal of Solid-state circuits.*,10,2533-2549., DOI: 10.1109/JSSC.2017.2717922,2017
- Li, W. yao., Yan, Chong. Wei., Zou, Zheng. Wei., et al.: Research progress of transient electromagnetic apparatus, *Journal of YunNan university (natural science edition).*, 34,233-241. 2012.
- Liu, H., Wang, W. D., Xiang, C. L., Han, L. J., Nie, H. Z.: A de-noising method using the improved wavelet threshold function based on
260 noise variance estimation ,*Mechanical System and Signal Processing.*, 99,30-46, DOI: 10.1016/j.ymssp.2017.
- Liu, J. N., Ai, W., Wen, F., Liu, D. H.: Design of Cascaded Multi-channel Signal Isolated Acquisition Circuit, *Instrument Technique and Sensor.*, 12,148-151,180 ,2016.
- Joo, S., Kim, S.: PSR enhancement techniques for output-capacitor-free LDO regulator design, *Analog Integrated Circuits and signal Processing.*, 2:319-327, DOI: 10.1007/s10470-017-1045-9, 2017.
- 265 Khomutov, S. Y., Mandrikova, O. V., Budilova, E. A., Arora, K.; Manjula, L.: Noise in raw data from magnetic observatories, *Geoscientific Instrumentation Methods and Data Systems.*,2,329-343. DOI:10.5194/gi-6-329-2017,2017.
- Oballe-Peinado, O, Hidalgo-Lopez, JA, Castellanos-Ramos, J, Sanchez-Duran, JA , Navas-Gonzalez, R, Herran, J, Vidal-Verdu, F.: FPGA-Based Tactile Sensor Suite Electronics for Real-Time Embedded Processing, *IEEE Transactions on industrial electronics.*, 12,9657-9665, DOI: 10.1109/TIE.2017.2714137, 2017.
- 270 Qi, Y. F., Yin, C. C., Wang, R., and Cai, J.: Mutlti-Transient EM full-time forward modeling and inversion of m-sequences, *Chinese J. Geophys.*, 7,2566-2577, doi:10.6038/cjg20150731.2015.
- Ren, Z. D., Guo, C. S., Lin, P. F.: Design of High-Performance LDO with Buffer Impedance Attenuation, *Microelectronics.*,2,225-227,232,2015.
- Wang, H. F., Chen, S. D., Zhang, S. Yuan, Z. W., Zhang, H. Y., Fang, D., Zhu, J.: A High-Performance Portable Transient Electro-Magnetic
275 Sensor for Unexploded Ordnance Detection, *Sensors (Basel, Switzerland).*, 11,DOI:10.3390/s17112651,2017.
- Wang, X. L., Gao, J. X., Tian, J. S., and Zhang, Y. T.: Design of power transformer in MTEM transmitter power, *Atlantis Press.*, 161–164, <https://doi.org/10.2991/cmes-15.2015.47>, 2015.
- Xue, G. Q., Chen, W. Y., Zhou, N. N., Li, Hai.: Short offset TEM technique with a grounded wire source for deep sounding, *Chinese J. Geophys.*,1:255-261,doi:10.6038/cjg20130126,2013.

- 280 Yun, S. J., Kim, J. S., Kim, Y. S.: Capless LDO Regulator Achieving -76 dB PSR and 96.3 fs FOM, IEEE Transactions on Circuits and Systems II-Express Briefs., 10, 1147-1151. DOI: 10.1109/TCSII.2016.2628965, 2017.
- Zhang, X. H., Du, J. L., Fan, C. G., Liu, D., Fang, J. L., Wang, L. S.: A Wireless Sensor Monitoring Node Based on Automatic Tracking Solar-Powered Panel for Paddy Field Environment, IEEE Internet of Things Journal., 5, 1304-1311. DOI: 10.1109/JIOT.2017.2706418, 2017.
- Zhang, X.Y., Zhang, Q.S., Wang, M., Kong, Q., Zhang, S.Q., He, R.H., Liu, S.H., Li, S.H., Yuan, Z.Z.: Development of a full-waveform voltage and
 285 current recording device for multichannel transient electromagnetic transmitters, Geoscientific Instrumentation Methods And Data Systems., 2, 495-503, DOI: 10.5194/gi-6-495, 2017.
- Zhong, H. S., Xue, G. Q., Li, X., Zhi, Q. Q., and Di, Q. Y.: Pseudo wave field extraction in the multi-channel transient electromagnetic (MTEM) method, Chin. J. Geophys., 59, 4424-4431, 2016.
- Zhou, N. N., Xue, G. Q., Chen, W. Y., Chen, J. L.: Large-depth hydrogeological detection in the North China-type coalfield through short-
 290 offset grounded-wire TEM, Environmental Earth Sciences., 3, 2393-22404. DOI: 10.1007/s12665-015-4240-y, 2015.
- Ziolkowski A, Parr R, Wright D, Nockles, V., Limond, C., Morris, E., Linfoot, J.: Multi-transient electromagnetic repeatability experiment over the North Sea Harding field. Geophysical Prospecting., 58, 1159-1176, 2010.